Embedded Triply Periodic Zero Mean Curvature Surfaces of Mixed Type in Lorentz–Minkowski 3-Space

Shoichi Fujimori, Wayne Rossman, Masaaki Umehara, Kotaro Yamada, & Seong-Deog Yang

1. Introduction

In any robust surface theory, it is essential to have a large collection of interesting examples. An interesting class of surfaces to study is the zero-mean curvature surfaces of mixed type in the Lorentz–Minkowski three-space $\mathbf{R}_1^3$, which, roughly speaking, are smooth surfaces of mixed causal type with mean curvature, wherever well-defined, equal to zero.

Several authors have found examples of such surfaces [12; 6; 14; 11; 3; 4], all having simple topology. The main goal of this article is to provide a concrete example of a family of such surfaces with nontrivial topology.

The motivation for the method of our construction is the fact that fold singularities of spacelike maximal surfaces have real analytical extensions to timelike minimal surfaces (see [6; 7; 8; 11; 9; 4], and, especially, [4], which is an expository article on this subject). Main ingredients are the spacelike maximal analogues in $\mathbf{R}_1^3$ of the Schwarz P surfaces and the Schwarz D surfaces in $\mathbf{R}^3$, which were remarked upon in the previous work [5] by the authors. The Schwarz P-type maximal surfaces admit cone-like singularities, whereas the Schwarz D-type maximal surfaces admit fold singularities (cf. Figure 1). By extending the Schwarz D-type (spacelike) maximal surfaces to timelike minimal surfaces, we obtain the following main result of this article.

Theorem A. *The one-parameter family of Schwarz D-type spacelike maximal surfaces $\{X_a\}_{0<a<1}$ has a unique analytic extension*

$$\tilde{X}_a : \Sigma_a \to \mathbf{R}_1^3/\Gamma_a \quad (0 < a < 1)$$

to embedded zero-mean-curvature surfaces, where $\mathbf{R}_1^3/\Gamma_a$ is a torus given by a suitable three-dimensional lattice Γ_a, and Σ_a is a closed orientable 2-manifold of genus three (*cf. Figure* 2).
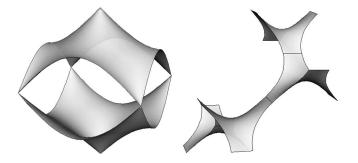
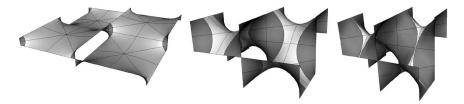**Figure 1**   Schwarz P-type (left) and D-type maximal surfaces (right)

Figure 2   Embedded triply periodic zero-mean curvature-surfaces of mixed type constructed in this article for $a = 0.1$ (left), $a = (\sqrt{3} - 1)/\sqrt{2} \approx 0.52$ (center), and $a = 0.9$ (right). The spacelike parts are indicated by grey shades, and the timelike parts are indicated by black shades

In so doing, we provide a concrete description of the family of triply periodic maximal surfaces containing the Schwarz P-type and D-type maximal surfaces.

2. Triply Periodic Maximal Surfaces

In this section, we construct triply periodic maximal surfaces in $\mathbf{R}_1^3$ based on the Schwarz P and D minimal surfaces in $\mathbf{R}^3$. We use either t, x, y or x_0, x_1, x_2 to denote the standard coordinates of $\mathbf{R}_1^3$.

Take the hyperelliptic Riemann surface

$$M_a := \{(z, w) \in (\mathbf{C} \cup \{\infty\})^2; w^2 = z^8 + (a^4 + a^{-4})z^4 + 1\}$$

of genus 3, where $a \in (0, 1)$ is a real constant. Take the Weierstrass data

$$G := z, \qquad \eta_\theta := e^{i\theta}\frac{dz}{w} \quad \left(\theta \in [0, \pi), i := \sqrt{-1}\right)$$

on M_a, and set

$$\hat{f}_{a,\theta} := \mathrm{Re} \int (1 - G^2, i(1 + G^2), 2G)\eta_\theta. \tag{2.1}$$

Then $\hat{f}_{a,\theta}$ gives a minimal surface in $\mathbf{R}^3$. When $a = (\sqrt{3} - 1)/\sqrt{2}$, that is, when $a^4 + a^{-4} = 14$, $\hat{f}_{a,0}$ (resp. $\hat{f}_{a,\pi/2}$) is called the *Schwarz P surface* (resp. the

Schwarz D surface). Also, for $a \in (0, 1)$, $\hat{f}_{a,0}$ (resp. $\hat{f}_{a,\pi/2}$) is called the *Schwarz P family* (resp. the *Schwarz D family*). For the period computation for those minimal surfaces, we refer to [13].

Now, for the same Riemann surface M_a and the Weierstrass data (G, η_θ) as above, we set

$$f_{a,\theta} := \operatorname{Re} \int \Phi_\theta : \widetilde{M}_a \longrightarrow \mathbf{R}_1^3,$$

where

$$\Phi_\theta := (-2G, 1 + G^2, i(1 - G^2))\eta_\theta. \tag{2.2}$$

Then $f_{a,\theta}$ gives a *maxface* (i.e. a maximal surface with admissible singularities, see [4] and [15]) in the Lorentz–Minkowski 3-space $\mathbf{R}_1^3$ of signature $(-, +, +)$. A point $p \in M_a$ is a singular point if and only if $|G(p)| = 1$, and a singular point p is a cuspidal edge point if and only if $\operatorname{Im}(dG/(G^2\eta)) \neq 0$ at p (see [5, Fact 1.3]). Using this, one can easily check that $f_{a,\theta}$ admits only cuspidal edge singularities whenever $\theta \neq 0, \pi/2$ for each $a \in (0, 1)$. On the other hand, if $\theta = 0$, then $f_{a,0}$ admits only cone-like singularities (see [5, Lemma 2.3]). Later, we will show that $f_{a,0}$ is triply periodic. Since $f_{a,0}$ has the same Weierstrass data as the Schwarz P surface in the Euclidean 3-space, we call $f_{a,0}$ the *Schwarz P-type maximal surface*.

As pointed out in [10, Definition 2.1] and [4, Proposition 2.14], there exists a duality between fold singularities and generalized cone-like singularities via conjugation of maximal surfaces. Since $f_{a,\pi/2}$ is the conjugate surface of $f_{a,0}$, we can conclude that $f_{a,\pi/2}$ admits only fold singularities (see [4]). Later, we also show that $f_{a,\pi/2}$ is triply periodic. Since $f_{a,\pi/2}$ has the same Weierstrass data as the Schwarz D surface in the Euclidean 3-space, we call $f_{a,\pi/2}$ the *Schwarz D-type maximal surface*.

The surface $f_{a,0}$ has the following symmetries.

LEMMA 2.1. *It holds that*

$$\varphi_1^*(\Phi_0)^T = \begin{pmatrix} 1 & 0 & 0 \\ 0 & 1 & 0 \\ 0 & 0 & -1 \end{pmatrix} \overline{(\Phi_0)}^T, \qquad \varphi_2^*(\Phi_0)^T = \begin{pmatrix} -1 & 0 & 0 \\ 0 & -1 & 0 \\ 0 & 0 & -1 \end{pmatrix} (\Phi_0)^T,$$

$$\varphi_3^*(\Phi_0)^T = \begin{pmatrix} -1 & 0 & 0 \\ 0 & 0 & 1 \\ 0 & -1 & 0 \end{pmatrix} (\Phi_0)^T, \qquad \varphi_4^*(\Phi_0)^T = \begin{pmatrix} -1 & 0 & 0 \\ 0 & -1 & 0 \\ 0 & 0 & 1 \end{pmatrix} (\Phi_0)^T,$$

where $(\Phi_0)^T$ is the transpose of Φ_0, and $\varphi_j^*(\Phi_0)^T$ $(j = 1, 2, 3, 4)$ is the pull-back of the $\mathbf{C}^3$-valued 1-form $(\Phi_0)^T$ by the maps $\varphi_j : M_a \to M_a$ given by

$$\varphi_1(z, w) := (\bar{z}, \bar{w}), \qquad \varphi_2(z, w) := (z, -w),$$

$$\varphi_3(z, w) := (iz, w), \qquad \varphi_4(z, w) := \left(\frac{1}{z}, \frac{w}{z^4}\right).$$

In the following discussion, we apply only the symmetry with respect to φ_3. Using this, we examine the period of $f_{a,\theta}$. We set

$$b := a^4 + a^{-4}.$$

We define the following four oriented regular arcs on M_a:

$$c_1(t) := \left(-it, \sqrt{t^8 + bt^4 + 1}\right), \quad t \in [-\infty, 0],$$

$$c_2(t) := \left(t, \sqrt{t^8 + bt^4 + 1}\right), \quad t \in [0, +\infty],$$

$$c_3(t) := \left(-it, \sqrt{t^8 + bt^4 + 1}\right), \quad t \in [-1, 1],$$

$$c_4(t) := \left(e^{it}, -e^{2it}\sqrt{2\cos 4t + b}\right), \quad t \in \left[-\frac{\pi}{2}, \frac{\pi}{2}\right],$$

where all the four square roots take positive real values. We then define two oriented loops $\gamma_1 : [-\infty, +\infty] \to M_a$ and $\gamma_2 : [-2, \pi] \to M_a$ by

$$\gamma_1(s) := \begin{cases} c_1(s) & \text{if } s \in [-\infty, 0], \\ c_2(s) & \text{if } s \in [0, \infty]; \end{cases} \tag{2.3}$$

$$\gamma_2(s) := \begin{cases} c_3(s+1) & \text{if } s \in [-2, 0], \\ c_4(s - \pi/2) & \text{if } s \in [0, \pi]. \end{cases}$$

The fundamental group $\pi_1(M_a)$ of M_a is generated by eight loops

$$\gamma_k, \quad \varphi_3 \circ \gamma_k, \quad (\varphi_3)^2 \circ \gamma_k := \varphi_3 \circ \varphi_3 \circ \gamma_k, \quad (\varphi_3)^3 \circ \gamma_k := \varphi_3 \circ \varphi_3 \circ \varphi_3 \circ \gamma_k$$
$$(k = 1, 2).$$

One can easily prove the next lemma following the computations in [13].

LEMMA 2.2. *We have*

$$\oint_{\gamma_1} \Phi_0 = (-q_1(a), q_2(a), q_2(a)), \qquad \oint_{\gamma_2} \Phi_0 = (iq_3(a), -iq_4(a), q_2(a)),$$

where $q_j(a)$ $(j = 1, 2, 3, 4)$ are positive real numbers given by

$$q_1(a) := \int_0^\infty \frac{4\,ds}{\sqrt{(b+2)s^4 - 2(b-6)s^2 + b + 2}} = \int_0^1 \frac{8t}{\sqrt{t^8 + bt^4 + 1}}\,dt,$$

$$q_2(a) := \int_0^\infty \frac{ds}{\sqrt{s^4 + s^2 + (b+2)/16}} = \int_0^1 \frac{2(1+t^2)}{\sqrt{t^8 + bt^4 + 1}}\,dt,$$

$$q_3(a) := \int_0^\infty \frac{4\,ds}{\sqrt{(b+2)s^4 + 2(b-6)s^2 + b + 2}} = \int_{-\pi/2}^{\pi/2} \frac{2\,dt}{\sqrt{2\cos 4t + b}},$$

$$q_4(a) := \int_0^\infty \frac{ds}{\sqrt{s^4 - s^2 + (b+2)/16}}.$$

We define two 3×4 matrices

$$P_k := \mathrm{Re}\left(\oint_{\gamma_k} e^{i\theta}(\Phi_0)^T, \oint_{\varphi_3 \circ \gamma_k} e^{i\theta}(\Phi_0)^T, \right.$$

$$\left. \oint_{(\varphi_3)^2 \circ \gamma_k} e^{i\theta}(\Phi_0)^T, \oint_{(\varphi_3)^3 \circ \gamma_k} e^{i\theta}(\Phi_0)^T \right)$$

for $k = 1, 2$. Then $f_{a,\theta}$ is triply periodic if and only if the eight column vectors of (P_1, P_2) belong to some lattice of $\mathbf{R}_1^3$.

Now we consider the case where $\theta = 0$. Since

$$\oint_{(\varphi_3)^j \circ \gamma_k} (\Phi_0)^T = \oint_{\gamma_k} ((\varphi_3)^j)^*(\Phi_0)^T \quad (j = 1, 2, 3; k = 1, 2),$$

Lemma 2.1 yields that

$$P_1|_{\theta=0} = \begin{pmatrix} -q_1 & q_1 & -q_1 & q_1 \\ q_2 & q_2 & -q_2 & -q_2 \\ q_2 & -q_2 & -q_2 & q_2 \end{pmatrix}, \tag{2.4}$$

$$P_2|_{\theta=0} = \begin{pmatrix} 0 & 0 & 0 & 0 \\ 0 & q_2 & 0 & -q_2 \\ q_2 & 0 & -q_2 & 0 \end{pmatrix}, \tag{2.5}$$

where $q_j = q_j(a)$ $(j = 1, \ldots, 4)$ are as in Lemma 2.2. Since each column vector of $P_1|_{\theta=0}$ and $P_2|_{\theta=0}$ is contained in the lattice

$$\Lambda := \left\{ m_0 \begin{pmatrix} q_1 \\ 0 \\ 0 \end{pmatrix} + m_1 \begin{pmatrix} 0 \\ q_2 \\ 0 \end{pmatrix} + m_2 \begin{pmatrix} 0 \\ 0 \\ q_2 \end{pmatrix} ; m_0, m_1, m_2 \in \mathbf{Z} \right\}, \tag{2.6}$$

the surface

$$f_{a,0} : M_a \longrightarrow \mathbf{R}_1^3/\Lambda$$

gives a maximal surface for all $a \in (0, 1)$. The left-hand side of Figure 1 is the figure of $f_{a,0}$ for $a = (\sqrt{3} - 1)/\sqrt{2}$.

Now we consider the case where $\theta = \pi/2$. By similar computations we have that

$$P_1|_{\theta=\pi/2} = O, \qquad P_2|_{\theta=\pi/2} = \begin{pmatrix} -q_3 & q_3 & -q_3 & q_3 \\ q_4 & 0 & -q_4 & 0 \\ 0 & -q_4 & 0 & q_4 \end{pmatrix}.$$

Since each column of $P_2|_{\theta=\pi/2}$ is contained in the lattice

$$\Lambda' := \left\{ m_0 \begin{pmatrix} q_3 \\ q_4 \\ 0 \end{pmatrix} + m_1 \begin{pmatrix} q_3 \\ 0 \\ q_4 \end{pmatrix} + m_2 \begin{pmatrix} q_3 \\ 0 \\ -q_4 \end{pmatrix} ; m_0, m_1, m_2 \in \mathbf{Z} \right\},$$

the surface

$$f_{a,\pi/2} : M_a \longrightarrow \mathbf{R}_1^3/\Lambda'$$

gives a maximal surface for all $a \in (0, 1)$. The right-hand side of Figure 1 corresponds to the figure of $f_{a,\pi/2}$ for $a = (\sqrt{3} - 1)/\sqrt{2}$.
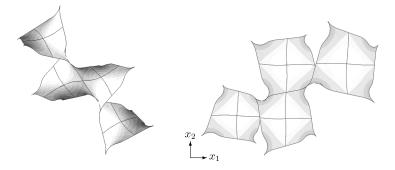
Figure 3 Two different views of the Gyroid-type maximal surface with $a \approx 0.346014$ and $\theta \approx 0.73073 \approx 41.8685°$ mentioned in Remark 2.3

REMARK 2.3. Numerical experiments suggest that there exists a triply periodic member in the family with $\theta \in (0, \pi/2)$, as an analogue of the Gyroid, which appears to have no self-intersections. See Figure 3. It would be interesting to theoretically confirm this observation.

REMARK 2.4. Here we consider the limit of $f_{a,\theta}$ as $a \to 1$. The Riemann surface M_a collapses to two spheres with four singular points at $(z, w) = (\pm e^{\pm \pi i/4}, 0)$, and the limit of $f_{a,\theta}$ is divided into two congruent maximal surfaces with the Weierstrass data

$$G = z, \qquad \eta_\theta = \pm e^{i\theta} \frac{dz}{z^4 + 1} \quad (\theta \in [0, \pi))$$

on $M' := (\mathbf{C} \cup \{\infty\}) \setminus \{\pm e^{\pm \pi i/4}\}$. The limit of $f_{a,0}$ is a subset of the triply periodic real analytic maximal surface

$$\mathcal{S}_+ := \{(t, x, y) \in \mathbf{R}_1^3; \cos t = \cos x \cos y\}$$

called *spacelike Scherk surface,* which contains singular lightlike lines (see [2] and [4] for the whole figure of $\mathcal{S}_+$). On the other hand, the limit of $f_{a,\pi/2}$ is a subset of the zero-mean-curvature entire graph

$$\mathcal{S}_0 := \{(t, x, y) \in \mathbf{R}_1^3; e^t \cosh x = \cosh y\},$$

given by Osamu Kobayashi [12] (see also [2] and [4]). $\mathcal{S}_0$ also contains four disjoint timelike minimal surfaces as subsets. See Figure 4.

REMARK 2.5. Here we consider the limit of $f_{a,\theta}$ as $a \to 0$. We first rescale the surface as $\sqrt{a^4 + a^{-4}} f_{a,\theta}$ and then take the limit as $a \to 0$. The Riemann surface M_a collapses as $a \to 0$ to two spheres with two singular points at $(z, w) = (0, 0)$, (∞, ∞), and the limit of $f_{a,\theta}$ is divided into two congruent maximal surfaces with the Weierstrass data

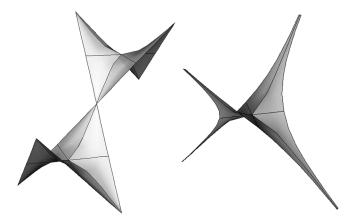$$G = z, \qquad \eta_\theta = \pm e^{i\theta} \frac{dz}{z^2} \quad (\theta \in [0, \pi))$$

Figure 4 The spacelike Scherk surface (left) and the spacelike part of the surface $\mathcal{S}_0$ in Remark 2.4 (right)
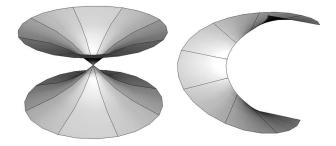

Figure 5 The spacelike elliptic catenoid (left) and the spacelike elliptic helicoid (right)

on $M' := \mathbf{C} \setminus \{0\}$. The limits of $f_{a,0}$ and of $f_{a,\pi/2}$ as $a \to 0$ are the *spacelike elliptic catenoid* and the *spacelike elliptic helicoid, respectively.* See Figure 5.

3. Analytic Extensions of Schwarz D-Type Maximal Surfaces to Triply Periodic Zero-Mean-Curvature Surfaces

When a maximal surface has fold singularities, we can analytically extend the maximal surface to a timelike surface with mean curvature zero. This fact has been observed in [4, Theorem 2.15]. In the previous section, we observed that the Schwarz D-type surface $f_{a,\pi/2}$ admits only fold singularities for each $0 < a < 1$. The image of the singular set of $f_{a,\pi/2}$ is a lightlike curve

$$\gamma_a(s) := \int_0^s \xi_a(t)(1, -\cos t, -\sin t)\, dt$$

$$\left(\xi_a(t) := \frac{2}{\sqrt{2\cos 4t + a^4 + a^{-4}}} \right). \tag{3.1}$$

Then
$$\tilde{f}_a(u, v) := \frac{1}{2}(\gamma_a(u + v) + \gamma_a(u - v))$$
is a timelike minimal surface (that is, a timelike surface with mean curvature zero; see Figure 2) such that
$$\tilde{f}_a(u, 0) = \gamma_a(u), \tag{3.2}$$
and $\tilde{f}_a$ is the analytic extension of the maximal surface $f_{a,\pi/2}$ (see Section 2 of [4]).

The following assertion holds.

LEMMA 3.1. *The surface $\tilde{f}_a(u, v)$ is an immersion on $\mathbf{R} \times (0, \pi)$.*

Proof. Since
$$\frac{\partial \tilde{f}_a}{\partial u} = \frac{1}{2}(\gamma_a'(u + v) + \gamma_a'(u - v)), \qquad \frac{\partial \tilde{f}_a}{\partial v} = \frac{1}{2}(\gamma_a'(u + v) - \gamma_a'(u - v)),$$

(u, v) is a singular point of $\tilde{f}_a$ (that is, a point where $\tilde{f}_a$ is not an immersion) if and only if
$$\gamma_a'(u + v) = \xi_a(u + v)(1, -\cos(u + v), -\sin(u + v))$$
and
$$\gamma_a'(u - v) = \xi_a(u - v)(1, -\cos(u - v), -\sin(u - v))$$
are linearly dependent, where γ_a' is the derivative of the curve γ_a. The linear dependency of two vectors $\gamma_a'(u + v)$ and $\gamma_a'(u - v)$ is equivalent to the validity of the two equalities
$$\cos(u + v) = \cos(u - v) \quad \text{and} \quad \sin(u + v) = \sin(u - v),$$
that is, $v \equiv 0 \pmod{\pi}$, proving the lemma.   □

LEMMA 3.2. *The timelike surface $\tilde{f}_a$ contains three line segments. More precisely,*
(1) $\tilde{f}_a(u, \pi/2)$ $(u \in \mathbf{R})$ *is a straight line parallel to the x_0-axis;*
(2) $\tilde{f}_a(0, v)$ $(0 < v < \pi)$ *is a line segment parallel to the x_2-axis;*
(3) $\tilde{f}_a(\pi/4, v)$ $(0 < v < \pi)$ *is a line segment parallel to the line $\{x_0 = x_1 + x_2 = 0\}$.*

Proof. By (3.1),
$$\begin{aligned}
\frac{\partial \tilde{f}_a}{\partial u}\left(u, \frac{\pi}{2}\right) &= \frac{1}{2}\left(\gamma_a'\left(u + \frac{\pi}{2}\right) + \gamma_a'\left(u - \frac{\pi}{2}\right)\right) \\
&= \frac{1}{2}\xi_a\left(u + \frac{\pi}{2}\right)\left(1, -\cos\left(u + \frac{\pi}{2}\right), -\sin\left(u + \frac{\pi}{2}\right)\right) \\
&\quad + \frac{1}{2}\xi_a\left(u - \frac{\pi}{2}\right)\left(1, -\cos\left(u - \frac{\pi}{2}\right), -\sin\left(u - \frac{\pi}{2}\right)\right) \\
&= \xi_a(u)(1, 0, 0)
\end{aligned}$$

because $\xi_a(u + \pi/2) = \xi_a(u - \pi/2) = \xi_a(u)$. Thus, (1) is proved. Similarly, direct computations show that

$$\frac{\partial \tilde{f}_a}{\partial v}(0, v) = \frac{-2 \sin v}{\sqrt{2 \cos 4v + a^4 + a^{-4}}}(0, 0, 1),$$

$$\frac{\partial \tilde{f}_a}{\partial v}\left(\frac{\pi}{4}, v\right) = \frac{\sqrt{2} \sin v}{\sqrt{-2 \cos 4v + a^4 + a^{-4}}}(0, 1, -1).$$

Thus, (2) and (3) hold. □

Like minimal surfaces in $\mathbf{R}^3$, both spacelike maximal surfaces and timelike minimal surfaces have reflection principles as follows.

FACT 3.3 (cf. [1, Theorem 3.10] and [9, Lemmas 4.1 and 4.2]).

(1) *Suppose that a spacelike maximal surface contains a spacelike line. Then the surface is symmetric with respect to the line.*
(2) *Suppose that a spacelike maximal surface is perpendicular to a timelike plane. Then the surface is symmetric with respect to the plane.*
(3) *Suppose that a timelike minimal surface contains a spacelike line or a timelike line. Then the surface is locally symmetric with respect to the line.*
(4) *Suppose that a timelike minimal surface is perpendicular to a spacelike plane or a timelike plane. Then the surface is locally symmetric with respect to the plane.*

We know that $\tilde{f}_a(u, 0)$ $(u \in \mathbf{R})$ consists of fold singularities (cf. (3.2)). Since $\tilde{f}_a(u, \pi/2)$ $(u \in \mathbf{R})$ is a straight line, (3) of Fact 3.3 implies that each point of $\tilde{f}_a(u, \pi)$ $(u \in \mathbf{R})$ is also a fold singularity, and by Lemma 3.2 we can analytically extend $\tilde{f}_a$ to the Schwarz D-type maximal surface. Also, by Lemma 3.2 we can consider

$$\Omega_a^{\min} := \left\{ \tilde{f}_a(u, v) \in \mathbf{R}_1^3; 0 \le u \le \frac{\pi}{4}, 0 < v \le \frac{\pi}{2} \right\} \tag{3.3}$$

to be a fundamental piece of $\tilde{f}_a$ because the whole timelike minimal immersion $\tilde{f}_a(u, v)$ $(u \in \mathbf{R}, 0 < v < \pi)$ can be obtained by reflections of $\Omega_a^{\min}$. Note that by Lemma 3.1 $\Omega_a^{\min}$ is immersed. The boundary $\partial \Omega_a^{\min}$ of $\Omega_a^{\min}$ consists of three straight line segments

$$\mathcal{L}_A^{\min} := \left\{ \tilde{f}_a(0, v) \in \mathbf{R}_1^3; 0 < v \le \frac{\pi}{2} \right\},$$

$$\mathcal{L}_B^{\min} := \left\{ \tilde{f}_a\left(\frac{\pi}{4}, v\right) \in \mathbf{R}_1^3; 0 < v \le \frac{\pi}{2} \right\},$$

$$\mathcal{L}_C^{\min} := \left\{ \tilde{f}_a\left(u, \frac{\pi}{2}\right) \in \mathbf{R}_1^3; 0 \le u \le \frac{\pi}{4} \right\},$$

and the singular curve $\gamma_a(s)$ $(0 \le s \le \pi/4)$.

Proof of Theorem A. For simplicity, we denote $f_{a,\pi/2}$ by f_a, where $f_{a,\pi/2}$ was defined in Section 2.

By Lemma 2.1 and Fact 3.3 we can consider

$$\Omega_a^{\max} := \left\{ f_a(z) \in \mathbf{R}_1^3; 0 \le |z| < 1, 0 \le \arg z \le \frac{\pi}{4} \right\} \tag{3.4}$$

to be a fundamental piece of f_a. We note that $\Omega_a^{\max}$ is immersed. The boundary $\partial \Omega_a^{\max}$ of $\Omega_a^{\max}$ consists of two straight line segments, which correspond to

$$\{ z \in \mathbf{C}; 0 \le |z| < 1, \arg z = 0 \} \quad \text{and} \quad \left\{ z \in \mathbf{C}; a \le |z| < 1, \arg z = \frac{\pi}{4} \right\},$$

a planar curve, which corresponds to

$$\left\{ z \in \mathbf{C}; 0 \le |z| \le a, \arg z = \frac{\pi}{4} \right\},$$

and the singular curve $\gamma_a(s)$ ($0 \le s \le \pi/4$). We set

$$\Omega_a^1 := \Omega_a^{\max} \cup \left\{ \gamma_a(s); 0 \le s \le \frac{\pi}{4} \right\} \cup \Omega_a^{\min}. \tag{3.5}$$

Since $\Omega_a^{\max}$ and $\Omega_a^{\min}$ match analytically through $\gamma_a(s)$ ($0 \le s \le \pi/4$), Ω_a^1 is immersed (see [4, Section 2] for the details). We define

$$\mathcal{L}_A^{\max} := \{ f_a(z) \in \mathbf{R}_1^3; 0 \le |z| < 1, \arg z = 0 \},$$

$$\mathcal{L}_B^{\max} := \left\{ f_a(z) \in \mathbf{R}_1^3; a \le |z| < 1, \arg z = \frac{\pi}{4} \right\},$$

$$\mathcal{L}_C^{\max} := \left\{ f_a(z) \in \mathbf{R}_1^3; 0 \le |z| \le a, \arg z = \frac{\pi}{4} \right\}.$$

It can be easily checked that $\mathcal{L}_A^{\max}$ is parallel to the x_2-axis and $\mathcal{L}_B^{\max}$ is parallel to the line

$$\{ (x_0, x_1, x_2) \in \mathbf{R}_1^3; x_0 = 0, x_1 + x_2 = 0 \},$$

and $\mathcal{L}_C^{\max}$ is contained in a plane which is parallel to the plane

$$\{ (x_0, x_1, x_2) \in \mathbf{R}_1^3; x_1 = x_2 \}.$$

Thus, $\mathcal{L}_A^{\max}$ and $\mathcal{L}_A^{\min}$, as well as $\mathcal{L}_B^{\max}$ and $\mathcal{L}_B^{\min}$, are collinear.

We set $\mathcal{L}_A := \mathcal{L}_A^{\max} \cup \mathcal{L}_A^{\min}$ and $\mathcal{L}_B := \mathcal{L}_B^{\max} \cup \mathcal{L}_B^{\min}$. Then the image of the projection of the boundary $\partial \Omega_a^1$ of Ω_a^1 into the $x_1 x_2$-plane is an isosceles right triangle. See Figure 6. We denote this isosceles right triangle with its interior by Δ. We also denote the length of the segment $\mathcal{L}_C^{\min}$ by $|\mathcal{L}_C^{\min}|$.

We have already seen that Ω_a^1 is immersed. Furthermore, we have the following proposition, which will be proved in Section 4.

PROPOSITION 3.4. *For each $a \in (0, 1)$, Ω_a^1 is embedded and contained in the closure of a vertical prism over the isosceles right triangle Δ with height $|\mathcal{L}_C^{\min}|$.*

Now we extend Ω_a^1 by reflection with respect to the planar curve $\mathcal{L}_C^{\max}$. We denote the resulting surface by Ω_a^2, which is two copies of Ω_a^1. Then Ω_a^2 is also embedded, and the boundary consists of five straight line segments ($\mathcal{L}_B$ and its reflection are collinear). See Figure 7.
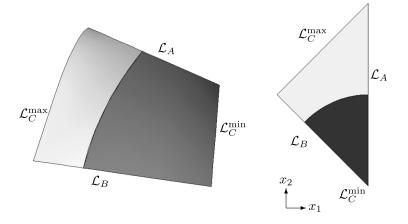
Figure 6 Left: Ω_a^1 defined in (3.5). The curve in the middle indicates the singular curve $\gamma_a(s)$, and the left-hand side (resp. right-hand side) is $\Omega_a^{\max}$ (resp. $\Omega_a^{\min}$). Right: Another view of Ω_a^1 such that the line $\mathcal{L}_C^{\min}$ is viewed as a single point at the bottom. On the top (resp. bottom) is $\Omega_a^{\max}$ (resp. $\Omega_a^{\min}$)
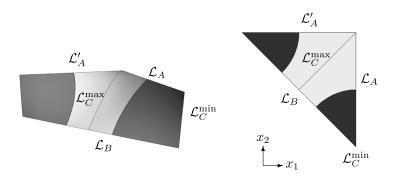

Figure 7 Left: Ω_a^2, that is, Ω_a^1 and its reflection with respect to the plane of $\mathcal{L}_C^{\max}$. The right-hand side of $\mathcal{L}_C^{\max}$ is Ω_a^1 and the left-hand side is its reflection. The spacelike parts are indicated by grey shades, and the timelike parts by black shades. Right: Another view of Ω_a^2. The right bottom (resp. left top) is Ω_a^1 (resp. its reflection)

We denote the reflection of $\mathcal{L}_A$ by $\mathcal{L}_A'$.

We extend Ω_a^2 by two more reflections with respect to $\mathcal{L}_A$ and $\mathcal{L}_A'$. We denote the resulting surface by Ω_a^8, which is four copies of Ω_a^2. Then Ω_a^8 is embedded, and the boundary consists of eight straight line segments (four (horizontal) spacelike line segments and four (vertical) timelike line segments). See Figure 8.

We now rotate Ω_a^8 with respect to the x_0 axis by angle $\pi/4$ so that the horizontal lines in the bottom (which are indicated by $\mathcal{L}_B$ in Figures 6 and 7) are
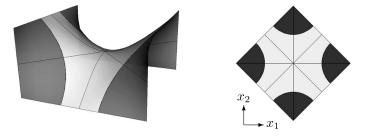
Figure 8 Left: Ω_a^8, that is, Ω_a^2 with its reflections with respect to $\mathcal{L}_A$ and $\mathcal{L}_A'$. Ω_a^2 is in the front. Right: Another view of Ω_a^8
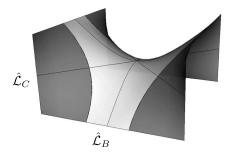

Figure 9 Ω_a^8 with labels $\hat{\mathcal{L}}_B$ and $\hat{\mathcal{L}}_C$

parallel to the x_1-axis. Then the boundary $\partial\Omega_a^8$ of Ω_a^8 consists of two (horizontal) line segments parallel to the x_1-axis in the bottom, two (horizontal) line segments parallel to the x_2-axis in the top, and four (vertical) line segments parallel to the x_0-axis. We label one of the (horizontal) line segments, parallel to the x_1-axis in the bottom, as $\hat{\mathcal{L}}_B$, and one of the (vertical) line segments, which is parallel to the x_0-axis and connects to $\hat{\mathcal{L}}_B$, as $\hat{\mathcal{L}}_C$. See Figure 9.

We denote the length of the segment $\hat{\mathcal{L}}_B$ (resp. $\hat{\mathcal{L}}_C$) by $|\hat{\mathcal{L}}_B|$ (resp. $|\hat{\mathcal{L}}_C|$). We extend Ω_a^8 by two more reflections with respect to $\hat{\mathcal{L}}_B$ and $\hat{\mathcal{L}}_C$. We denote the resulting surface by Ω_a^{32}, which is four copies of Ω_a^8. Then Ω_a^{32} is still embedded and is contained in the closure of a rectangular parallelepiped with height $2|\hat{\mathcal{L}}_C|$ over a square of side length $2|\hat{\mathcal{L}}_B|$. See Figure 10.

Then Ω_a^{32} and its translation by

$$(2\varepsilon_0|\hat{\mathcal{L}}_C|, 2\varepsilon_1|\hat{\mathcal{L}}_B|, 2\varepsilon_2|\hat{\mathcal{L}}_B|), \quad \text{where } \varepsilon_j = \pm 1 \ (j = 0, 1, 2),$$

match analytically since each translation can be obtained by a reflection with respect to some straight line. Therefore,

$$\Omega_a := \{\Omega_a^{32} + (2m_0|\hat{\mathcal{L}}_C|, 2m_1|\hat{\mathcal{L}}_B|, 2m_2|\hat{\mathcal{L}}_B|); m_0, m_1, m_2 \in \mathbf{Z}\} \subset \mathbf{R}_1^3$$
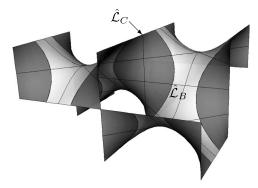
Figure 10 Ω_a^{32}, that is, Ω_a^8 with its reflections with respect to $\hat{\mathcal{L}}_B$ and $\hat{\mathcal{L}}_C$
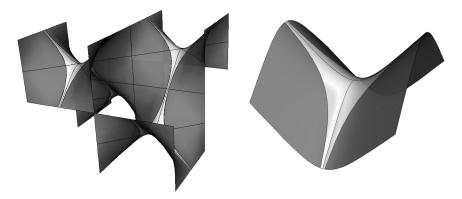

Figure 11 Ω_a^{32} with $a = 0.9$ (left) and its limit as $a \to 1$ (right)

is an embedded triply periodic surface. In other words, Ω_a^{32} is embedded in a torus $\mathbf{R}_1^3 / \Gamma_a$, where

$$\Gamma_a := \{(2m_0|\hat{\mathcal{L}}_C|, 2m_1|\hat{\mathcal{L}}_B|, 2m_2|\hat{\mathcal{L}}_B|) \in \mathbf{R}_1^3; m_0, m_1, m_2 \in \mathbf{Z}\}$$

is a lattice in $\mathbf{R}_1^3$.

We clearly see that this surface Ω_a is topologically the same as the Schwarz D minimal surface in $\mathbf{R}^3$ (see Figure 2). Thus, Ω_a^{32} in the quotient $\mathbf{R}_1^3 / \Gamma_a$ is a closed orientable 2-manifold of genus three. $\qquad\qquad\square$

REMARK 3.5. Here we consider the limit as $a \to 1$. In this case, we obtain the zero-mean-curvature entire graph

$$\mathcal{S}_0 = \{(t, x, y) \in \mathbf{R}_1^3; e^t \cosh x = \cosh y\},$$

which we already mentioned in Remark 2.4. See Figure 11. See also Figure 12 to compare this limiting behavior with that of the minimal surfaces in $\mathbf{R}^3$.
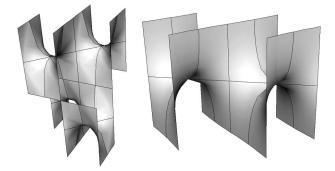
Figure 12   Schwarz D surface in $\mathbf{R}^3$ with $a = 0.9$ (left) and the doubly periodic Scherk surface in $\mathbf{R}^3$ as a limit of Schwarz D surface as $a \to 1$ (right)
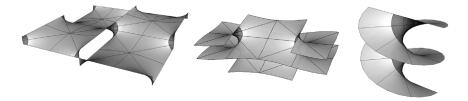

Figure 13 Ω_a^{32} in $\mathbf{R}_1^3$ with $a = 0.1$ (left), another view of Ω_a^{32} with $a = 0.1$ (center), and the limit as $a \to 0$ (right)
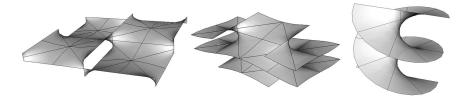

Figure 14   Schwarz D surface in $\mathbf{R}^3$ with $a = 0.1$ (left), another view of the Schwarz D surface in $\mathbf{R}^3$ with $a = 0.1$ (center), and the helicoid in $\mathbf{R}^3$ as a limit as $a \to 0$ with suitable rescaling of the Schwarz D surface (right)

REMARK 3.6. Here we consider the limit as $a \to 0$. We first multiply the surface by $\sqrt{a^4 + a^{-4}}$ to rescale the surface, as we did in Remark 2.5, and then take the limit as $a \to 0$. In this case, we obtain the zero-mean-curvature surface, which is exactly the same as the minimal helicoid in $\mathbf{R}^3$ [12]. See Figure 13. See also Figure 14 to compare the limiting behavior with that of the minimal surfaces in $\mathbf{R}^3$.

4. Proof of the Embeddedness

In this section we present a proof of Proposition 3.4.

We denote by $\Delta \times \mathcal{L}_C^{\min}$ the vertical prism over the isosceles right triangle Δ with height $|\mathcal{L}_C^{\min}|$ as in Proportion 3.4.

First, we prepare three lemmas.

LEMMA 4.1. *The piece of surface $\Omega_a^{\max}$ is embedded and contained in the closure $\overline{\Delta \times \mathcal{L}_C^{\min}}$ of $\Delta \times \mathcal{L}_C^{\min}$.*

Proof. The projection of $\Omega_a^{\max}$ into the x_1x_2-plane is represented by

$$\mathrm{Re} \int (1+z^2, i(1-z^2))i\, \frac{dz}{w} = \mathrm{Re} \int (i(1+z^2), -(1-z^2))\frac{dz}{w},$$

which is the same as the projection of the Schwarz P minimal surface in $\mathbf{R}^3$ (see (2.1)). So $\Omega_a^{\max}$ is a graph over the x_1x_2-plane. Since the boundary $\partial\Omega_a^{\max}$ of $\Omega_a^{\max}$ is contained in $\overline{\Delta \times \mathcal{L}_C^{\min}}$, $\Omega_a^{\max}$ itself is contained in $\overline{\Delta \times \mathcal{L}_C^{\min}}$ as well, by the maximum principle. Thus, $\Omega_a^{\max}$ is embedded and contained in $\overline{\Delta \times \mathcal{L}_C^{\min}}$.   □

LEMMA 4.2. *The projection of the singular curve $\gamma_a(s)$ $(0 \le s \le 2\pi)$ in (3.1) into the x_1x_2-plane is a closed convex curve.*

Proof. Let $(x_1(s), x_2(s))$ be the projection of $\gamma_a(s)$ into the x_1x_2-plane. It is trivial to see that $(x_1(s), x_2(s))$ is a closed C^∞-regular curve of rotation index one. Now we compute the curvature $\kappa_a(s)$ of $(x_1(s), x_2(s))$ and see that

$$\kappa_a(s) = \frac{\dot{x}_1(s)\ddot{x}_2(s) - \dot{x}_2(s)\ddot{x}_1(s)}{(\dot{x}_1^2(s) + \dot{x}_2^2(s))^{3/2}} = \sqrt{\xi_a(s)} > 0,$$

where ξ_a was defined in (3.1). So, $(x_1(s), x_2(s))$ is a convex curve.   □

LEMMA 4.3. *The intersection $\overline{\Omega_a^{\max}} \cap \overline{\Omega_a^{\min}} = \{\gamma_a(s); 0 \le s \le \pi/4\}$, where $\overline{\Omega_a^{\max}}$ (resp. $\overline{\Omega_a^{\min}}$) is the closure of $\Omega_a^{\max}$ (resp. $\Omega_a^{\min}$).*

Proof. We note that $\tilde{f}_a(u, v)$ is the midpoint of $\gamma_a(u + v)$ and $\gamma_a(u - v)$. Therefore, the projection of $\tilde{f}_a(u, v)$ into the x_1x_2-plane is the midpoint of the projections of $\gamma_a(u + v)$ and $\gamma_a(u - v)$ into the x_1x_2-plane. Hence, the projection of $\tilde{f}_a(u, v)$ into the x_1x_2-plane is inside the convex curve. The claim follows.   □

Thus, to prove Proposition 3.4, it suffices to show that $\Omega_a^{\min}$ is embedded and contained in the closure $\overline{\Delta \times \mathcal{L}_C^{\min}}$ of $\Delta \times \mathcal{L}_C^{\min}$, by the above three lemmas. To this end, we reparameterize γ_a and $\tilde{f}_a$ by their height as follows:

We define the diffeomorphism $\tau : \mathbf{R} \to \mathbf{R}$ by

$$\tau(s) := \int_0^s \xi_a(t)\, dt,$$

which is the height function (i.e. the x_0-component) of $\gamma_a(s)$. Using the inverse function $s = s(\tau)$ of $\tau(s)$, we define the parameter change

$$\tilde{\gamma}_a(\tau) := \gamma_a(s(\tau))$$

of $\gamma_a(s)$. We also define $(\alpha, \beta) : \mathbf{R}^2 \to \mathbf{R}^2$ by

$$(\alpha, \beta) = (\alpha(u, v), \beta(u, v)) := \left(\frac{\tau(u+v) + \tau(u-v)}{2}, \frac{\tau(u+v) - \tau(u-v)}{2} \right)$$

and

$$\check{f}_a(\alpha, \beta) := \frac{1}{2}(\tilde{\gamma}_a(\alpha + \beta) + \tilde{\gamma}_a(\alpha - \beta)).$$

Since $\tilde{\gamma}_a(\alpha \pm \beta) = \tilde{\gamma}_a(\tau(u \pm v)) = \gamma_a(u \pm v)$, we see that $\check{f}_a(\alpha, \beta)$ and $\tilde{f}_a(u, v)$ give the same surface (see [4, Proposition 2.2]). We set

$$c_a := \tau(\pi) = \int_0^\pi \xi_a(t)\, dt. \tag{4.1}$$

LEMMA 4.4. *Consider the map* $\psi : \mathbf{R} \times (0, \pi) \ni (u, v) \mapsto (\alpha, \beta) \in \mathbf{R} \times (0, c_a)$. *Then,* ψ *is a diffeomorphism, and the image of the rectangle*

$$0 \le u \le \frac{\pi}{4}, \qquad 0 \le v \le \frac{\pi}{2},$$

is again a rectangle, which is given by

$$0 \le \alpha \le \tau\left(\frac{\pi}{4}\right), \qquad 0 \le \beta \le \tau\left(\frac{\pi}{2}\right) = \frac{c_a}{2}.$$

Proof. It is easy to see that

$$(u, v) = \left(\frac{\tau^{-1}(\alpha + \beta) + \tau^{-1}(\alpha - \beta)}{2}, \frac{\tau^{-1}(\alpha + \beta) - \tau^{-1}(\alpha - \beta)}{2} \right)$$

gives the inverse function for ψ. Since the Jacobian

$$\frac{\partial(\alpha, \beta)}{\partial(u, v)} = \xi_a(u+v)\xi_a(u-v)$$

is always positive, ψ is a diffeomorphism.

Furthermore, we see that for any $n \in \mathbf{Z}$,

$$\beta(u, v) = \frac{1}{2}(\tau(u+v) - \tau(u-v)) = \frac{1}{2}\int_{u-v}^{u+v} \xi_a(t)\, dt,$$

$$\beta\left(u, \frac{n\pi}{2}\right) = \frac{1}{2}\int_{u-n\pi/2}^{u+n\pi/2} \xi_a(t)\, dt = \frac{1}{2}\int_0^{n\pi} \xi_a(t)\, dt = n\tau\left(\frac{\pi}{2}\right)$$

$$\left(\text{since } \xi_a(t) \text{ is periodic with period } \frac{\pi}{2}\right),$$

$$\alpha(0, v) = \frac{1}{2}\left(\int_0^v \xi_a(t)\, dt + \int_0^{-v} \xi_a(t)\, dt \right) = 0 \quad (\text{since } \xi_a(t) \text{ is even}),$$

$$\alpha\left(\frac{\pi}{4}, v\right) = \frac{1}{2}\left(\int_0^{\pi/4+v} \xi_a(t)\, dt + \int_0^{\pi/4-v} \xi_a(t)\, dt \right)$$

$$= \frac{1}{2}\left(\int_0^{\pi/4} + \int_{\pi/4}^{\pi/4+v} + \int_0^{\pi/4} + \int_{\pi/4}^{\pi/4-v}\right)\xi_a(t)\,dt$$

$$= \int_0^{\pi/4} \xi_a(t)\,dt = \tau\left(\frac{\pi}{4}\right),$$

from which the rest of the claim follows. □

By this lemma we have that

$$\Omega_a^{\min} = \left\{\check{f}_a(\alpha, \beta) \in \mathbf{R}_1^3; 0 \le \alpha \le \tau\left(\frac{\pi}{4}\right), 0 < \beta \le \tau\left(\frac{\pi}{2}\right)\right\}.$$

REMARK 4.5. The x_0-component of $\check{f}_a(\alpha, \beta)$ is α, that is,

$$x_0 \circ \check{f}_a(\alpha, \beta) = \frac{1}{2}\left(\int_0^{\alpha+\beta} dt + \int_0^{\alpha-\beta} dt\right) = \alpha.$$

Now we prove the embeddedness of $\Omega_a^{\min}$. In fact, we can prove the following stronger lemma.

LEMMA 4.6. *The surface $\check{f}_a(\alpha, \beta)$ ($\alpha \in \mathbf{R}, \beta \in (0, c_a)$) is embedded, where c_a was defined in* (4.1).

Proof. Suppose that $\check{f}_a(\alpha, \beta) = \check{f}_a(\alpha', \beta')$, where $\alpha, \alpha' \in \mathbf{R}$ and $\beta, \beta' \in (0, c_a)$. Then by Remark 4.5 we have $\alpha = \alpha'$. Suppose now that $\beta < \beta'$. Let $\pi_0 : \mathbf{R}_1^3 \ni (x_0, x_1, x_2) \mapsto (x_1, x_2) \in \mathbf{R}^2$ be the projection. By Lemma 4.2, $\pi_0 \circ \gamma_a(\tau)$ is a closed convex curve. Since $\pi_0 \circ \gamma_a(s)$ is 2π-periodic, we see that $\pi_0 \circ \tilde{\gamma}_a(\tau)$ is $2c_a$-periodic. Since $0 < \beta < \beta' < c_a$,

$$\pi_0 \circ \tilde{\gamma}_a(\alpha - \beta'), \quad \pi_0 \circ \tilde{\gamma}_a(\alpha - \beta), \quad \pi_0 \circ \tilde{\gamma}_a(\alpha),$$
$$\pi_0 \circ \tilde{\gamma}_a(\alpha + \beta), \quad \pi_0 \circ \tilde{\gamma}_a(\alpha + \beta')$$

lie on the curve $\pi_0 \circ \tilde{\gamma}_a(\tau)$ in this order. The assumption that $\check{f}_a(\alpha, \beta) = \check{f}_a(\alpha, \beta')$ implies that the midpoint of $\pi_0 \circ \tilde{\gamma}_a(\alpha - \beta')$ and $\pi_0 \circ \tilde{\gamma}_a(\alpha + \beta')$ is equal to the midpoint of $\pi_0 \circ \tilde{\gamma}_a(\alpha - \beta)$ and $\pi_0 \circ \tilde{\gamma}_a(\alpha + \beta)$, which is a contradiction by the convexity of $\pi_0 \circ \tilde{\gamma}_a(\tau)$. So, $\beta \ge \beta'$. In a similar way we can conclude $\beta' \ge \beta$, hence $\beta = \beta'$. This finishes the proof. □

Hence, proving the following lemma completes the proof of Proposition 3.4.

LEMMA 4.7. *The piece of surface $\Omega_a^{\min}$ is contained in the closure $\overline{\Delta \times \mathcal{L}_C^{\min}}$ of $\Delta \times \mathcal{L}_C^{\min}$.*

Proof. Direct computations show that

$$\frac{\partial \check{f}_a}{\partial \alpha} = (1, -2\cos u \cos v, -2\sin u \cos v),$$

$$\frac{\partial \check{f}_a}{\partial \beta} = (1, 2\sin u \sin v, -2\cos u \sin v).$$

Because $u \in (0, \pi/4)$, $v \in (0, \pi/2)$, we have

$$-2\cos u \cos v < 0, \quad -2\sin u \cos v < 0, \quad 2\sin u \sin v > 0, \quad -2\cos u \sin v < 0.$$

Since the boundary $\partial \Omega_a^{\min}$ of $\Omega_a^{\min}$ consists of the three straight line segments

$$\mathcal{L}_A^{\min} := \left\{ \check{f}_a(0, \beta) \in \mathbf{R}_1^3; 0 < \beta \le \frac{c_a}{2} \right\},$$

$$\mathcal{L}_B^{\min} := \left\{ \check{f}_a\left(\tau\left(\frac{\pi}{4}\right), \beta\right) \in \mathbf{R}_1^3; 0 < \beta \le \frac{c_a}{2} \right\},$$

$$\mathcal{L}_C^{\min} := \left\{ \check{f}_a\left(\alpha, \frac{c_a}{2}\right) \in \mathbf{R}_1^3; 0 \le \alpha \le \tau\left(\frac{\pi}{4}\right) \right\},$$

and the singular curve $\tilde{\gamma}_a(\tau)$ $(0 \le \tau \le \tau(\pi/4))$, all contained in $\overline{\Delta \times \mathcal{L}_C^{\min}}$, the claim follows. $\square$

References

[1] L. J. Alías, R. M. B. Chaves, and P. Mira, *Björling problem for maximal surfaces in Lorentz–Minkowski space,* Math. Proc. Cambridge Philos. Soc. 134 (2003), 289–316.

[2] S. Fujimori, Y. W. Kim, S.-E. Koh, W. Rossman, H. Shin, H. Takahashi, M. Umehara, K. Yamada, and S.-D. Yang, *Zero mean curvature surfaces in $\mathbf{L}^3$ containing a light-like line,* C. R. Acad. Paris, Ser. I 350 (2012), 975–978.

[3] S. Fujimori, Y. W. Kim, S.-E. Koh, W. Rossman, H. Shin, M. Umehara, K. Yamada, and S.-D. Yang, *Zero mean curvature surfaces in Lorentz–Minkowski 3-space which change type across a light-like line,* Osaka Math. J. (to appear).

[4] ———, *Zero mean curvature surfaces in Lorentz–Minkowski 3-space and 2-dimensional fluid mechanics,* Math. J. Okayama Univ. (to appear).

[5] S. Fujimori, W. Rossman, M. Umehara, K. Yamada, and S.-D. Yang, *New maximal surfaces in Minkowski 3-space with arbitrary genus and their cousins in de Sitter 3-space,* Results Math. 56 (2009), 41–82.

[6] C. Gu, *The extremal surfaces in the 3-dimensional Minkowski space,* Acta. Math. Sin. 1 (1985), 173–180.

[7] ———, *A global study of extremal surfaces in 3-dimensional Minkowski space,* Differential geometry and differential equations (Shanghai, 1985), Lecture Notes in Math., 1255, pp. 26–33, Springer, 1987.

[8] ———, *Extremal surfaces of mixed type in Minkowski space $\mathbf{R}^{n+1}$,* Variational methods (Paris, 1988), Progr. Nonlinear Differential Equations Appl., 4, pp. 283–296, Birkhäuser, Boston, 1990.

[9] Y. W. Kim, S.-E. Koh, H. Shin, and S.-D. Yang, *Spacelike maximal surfaces, timelike minimal surfaces, and Björling representation formulae,* J. Korean Math. Soc. 48 (2011), 1083–1100.

[10] Y. W. Kim and S.-D. Yang, *Prescribing singularities of maximal surfaces via a singular Björling representation formula,* J. Geom. Phys. 57 (2007), no. 11, 2167–2177.

[11] V. A. Klyachin, *Zero mean curvature surfaces of mixed type in Minkowski space,* Izv. Math. 67 (2003), 209–224.

[12] O. Kobayashi, *Maximal surfaces in the 3-dimensional Minkowski space $\mathbb{L}^3$,* Tokyo J. Math. 6 (1983), 297–309.

[13] M. Ross, *Schwarz' P and D surfaces are stable,* Differential Geom. Appl. 2 (1992), 179–195.

[14] V. Sergienko and V. G. Tkachev, *Doubly periodic maximal surfaces with singularities,* Proceedings on analysis and geometry (Russian) (Novosibirsk Akademgorodok, 1999), pp. 571–584, Izdat. Ross. Akad. Nauk Sib. Otd. Inst. Mat., Novosibirsk, 2000.

[15] M. Umehara and K. Yamada, *Maximal surfaces with singularities in Minkowski space,* Hokkaido Math. J. 35 (2006), 13–40.

S. Fujimori
Department of Mathematics
Okayama University
Tsushima-naka
Okayama 700-8530
Japan

fujimori@math.okayama-u.ac.jp

M. Umehara
Department of Mathematical and
   Computing Sciences
Tokyo Institute of Technology
2-12-1-W8-34, O-okayama
   Meguro-ku
Tokyo 152-8552
Japan

umehara@is.titech.ac.jp

S.-D. Yang
Department of Mathematics
Korea University
Seoul 136-701
Korea

sdyang@korea.ac.kr

W. Rossman
Department of Mathematics
Faculty of Science
Kobe University
Rokko, Kobe 657-8501
Japan

wayne@math.kobe-u.ac.jp

K. Yamada
Department of Mathematics
Tokyo Institute of Technology
1-12-1-H-7, O-okayama, Meguro-ku
Tokyo 152-8551
Japan

kotaro@math.titech.ac.jp